

## Comparative Analysis of the Multicenter, Long Bond in [TCNE]<sup>-</sup> and Phenalenyl Radical Dimers: A Unified Description of Multicenter, Long Bonds

Fernando Mota,<sup>†</sup> Joel S. Miller,<sup>\*,‡</sup> and Juan J. Novoa<sup>\*,†</sup>

*Departament de Química Física & IQTCUB Facultat de Química, Universitat de Barcelona, Avenida Diagonal, 647, 08028-Barcelona, Spain, and Department of Chemistry, University of Utah, Salt Lake City, Utah 84112-0850*

Received January 14, 2009; E-mail: juan.novoa@ub.edu; jsmiller@chem.utah.edu

**Abstract:** The nature of the multicenter, long bond in neutral phenalenyl dimers is analyzed in detail and compared to the multicenter, long bond in [TCNE]<sub>2</sub><sup>2-</sup>. These dimers are prototypes of multicenter, long bond in dimers of neutral and anion radicals. This was done by examining the number of electrons (*m*) and atomic centers (*c*) involved in the long bond for these dimers, as well as identifying the dominant attractive components of their interaction energy (SOMO–SOMO bonding, dispersion, and the sum of the exchange–repulsion and electrostatic components) in accord with Pauling’s focus on total bond energies. The long bond in [TCNE]<sub>2</sub><sup>2-</sup> is a 2e<sup>-</sup>/4c bond, the electrostatic component is repulsive, and the dominant attractive component is the dispersion component (–27.7 kcal/mol), about two times larger than the bonding component. In phenalenyl dimers the dispersion component (–31.7 kcal/mol) is about 2.5 times stronger (than the SOMO–SOMO bonding component; hence, the multicenter, long bond in these dimers is closer to a van der Waals bond than to a covalent bond. Consequently, it possesses a two-electrons/fourteen center 2e<sup>-</sup>/14c bond, rather than the 2e<sup>-</sup>/12c bond suggested by the SOMO–SOMO bonding component. The covalent-like properties in phenalenyl dimers result from the dominant dispersion component that enable the fragments to approach each other so that their SOMOs overlap and produce a qualitative MO diagram identical to that found in conventional covalent bonds.

### Introduction

Long, multicenter bonding was first introduced to describe the structure and electronic and magnetic properties (e.g., diamagnetism, UV and IR spectra) of dimers of the [TCNE]<sup>-</sup> (TCNE = tetracyanoethylene) anion-radical, [TCNE]<sup>-</sup><sub>2</sub><sup>2-</sup> (Figure 1).<sup>1</sup> Subsequently the dimer of the neutral 2,5,8-tri-*t*-butylphenalenyl<sup>2,3</sup> (**1**, for convenience we will also refer to this dimer as the phenalenyl dimer), and the dimers of the [TTF]<sup>+</sup> cation radical<sup>4</sup> have been reported. These bonds have all the properties associated with covalent bonds, except that (a) their distance is much longer than that for the conventional covalent C–C bonds (≤1.54 Å) but shorter than the sum of two carbon van der Waals radii (3.4 Å), and (b) the stability

of the dimers, where they are found, does not originate from the SOMO–SOMO overlap energetic component but from other components (i.e., electrostatic cation⋯anion interactions in [TCNE]<sup>-</sup><sub>2</sub><sup>2-</sup> dimers<sup>1</sup>). Long, multicenter bonds have also been reported in the solid state and in solution.<sup>1–4</sup> Although most of the long bonds reported to date are multicentered (i.e., involve more than two atomic centers), not all known long bonds are necessarily multicenter bonds.<sup>1</sup>

The stability of the long bond in ionic radical dimers in the solid state was shown to originate partially from the electrostatic cation–anion interactions and, and to a lesser extend by an ion-radical⋯ion-radical dispersion component.<sup>1–5</sup> In solution, the attractive cation<sup>+</sup>⋯anion<sup>-</sup> interactions are substituted by ion⋯solvent interactions.<sup>4,6</sup> These conclusions are based on theoretical studies on isolated π-[TCNE]<sub>2</sub><sup>2-</sup> and π-[TTF]<sub>2</sub><sup>2+</sup> dimers<sup>1,4</sup> that showed that both types of ion-radical dimers are energetically unstable when isolated. Using computational methods that do not include the dispersion energetic component (e.g., the Hartree–Fock method) the electrostatic repulsion (*E*<sub>elec</sub>, mainly originating from the net charge on the interacting fragments) exceeds the SOMO–SOMO bonding component (*E*<sub>bond</sub>, originating from the SOMO–SOMO overlap), both being properly accounted for by the Hartree–Fock method. Using methods that make a proper evaluation of the dispersion

<sup>†</sup> Universitat de Barcelona.

<sup>‡</sup> University of Utah.

- (1) Novoa, J. J.; Lafuente, P.; Del Sesto, R. E.; Miller, J. S. *Angew. Chem., Int. Ed.* **2001**, *40*, 2540. Del Sesto, R. E.; Miller, J. S.; Novoa, J. J.; Lafuente, P. *Chem.–Eur. J.* **2002**, *8*, 4894. Novoa, J. J.; Lafuente, P.; Del Sesto, R. E.; Miller, J. S. *CrystEngComm* **2002**, *4*, 373. Miller, J. S.; Novoa, J. J. *Acc. Chem. Res.* **2007**, *40*, 189.
- (2) Goto, K.; Kubo, T.; Yamamoto, K.; Nakasuji, K.; Sato, K.; Shiomi, D.; Takui, T.; Kubota, M.; Kobayashi, T.; Yakusi, K.; Ouyang, J.; Nakasuji, K. *J. Am. Chem. Soc.* **1999**, *121*, 1619.
- (3) Small, D.; Zaitsev, V.; Jung, Y.; Rosokha, S. V.; Head-Gordon, M.; Kochi, J. K. *J. Am. Chem. Soc.* **2004**, *126*, 13850. (b) Small, D.; Rosokha, S. V.; Kochi, J. K.; Head-Gordon, M. *J. Phys. Chem. A* **2005**, *109*, 11261. Zaitsev, V.; Rosokha, S. V.; Head-Gordon, M.; Kochi, J. K. *J. Org. Chem.* **2006**, *71*, 520.
- (4) Garcia-Yoldi, I.; Miller, J. S.; Novoa, J. J. *J. Phys. Chem. A*, **2009**, *113*, 484.

(5) Bock, H.; Ruppert, K.; Fenske, D.; Goesmann, H. *Z. Anorg. Allg. Chem.* **1991**, *595*, 275.

(6) Jakowski, J.; Simons, J. *J. Am. Chem. Soc.* **2003**, *125*, 16089.

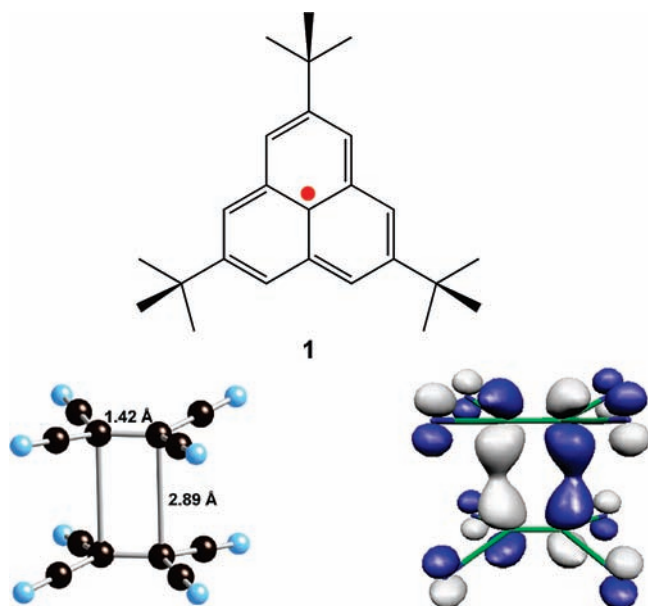


**Figure 1.** Structure of the  $\pi$ -[TCNE] $_2^{2-}$  dimer in its  $L_c$  conformation found in  $K_2$ [TCNE] $_2$ (glyme) $_2$  [5] (left);  $b_{2u}$  HOMO for the  $2e^-/4c$  long bond covalent-like properties in the  $\pi$ -[TCNE] $_2^{2-}$  dimer (right).

component,<sup>7</sup> the interior long bonds are further stabilized, making the isolated ion radicals dimers slightly metastable, although still less stable than the dissociated monomers. These studies also demonstrated that long bonds between ion radical pairs differ from covalent bonds in (a) the origin of their energetic stability and (b) their equilibrium distance. Note that these long bonds also differ from van der Waals bonds, as they involve open-shell charged interacting fragments and consequently possess a dominant electrostatic energetic component (complemented by a smaller SOMO–SOMO overlap component). They are also different from ionic bonds, due to the existence of a SOMO–SOMO overlap component. Nonetheless, they share some of the properties of each of covalent, van der Waals, and ionic bonds.

The electronic structure of species that exhibit long bonds is also important to understand their properties. The electronic structure can be represented using the typical MO diagram, which in the case of a dimer depicts the changes in the molecular orbital shape and energies as the fragments orbitals are allowed to overlap. The most important information about these MO diagrams can be described in a compact form by indicating the number of electrons ( $m$ ) and atomic centers ( $n$ ) that participate in the bond. This enables them to be identified as an  $m$ -electrons/ $n$ -centers bond,<sup>1</sup>  $me^-/nc$ . For instance, the H–H bond present in  $H_2$  can be classified as a  $2e^-/2c$  bond, which summarizes the main aspects of the electronic changes that take place as the H–H is formed. This classification provides a “quick view” of the most relevant aspect of the electronic structure responsible for the energetic stability and covalent-like properties of long, multicenter bonds. In our initial work on the  $\pi$ -[TCNE] $_2^{2-}$  dimers, we classified its long bond as a  $2e^-/4c$  bond, with the two electrons being the unpaired electrons from each [TCNE] $^{\cdot-}$ , and are delocalized over the four central  $sp^2$ -C atoms found in

**Table 1.** Values of  $E_{int}$ ,  $E_{er}$ ,  $E_{el}$ ,  $E_{pol}$ ,  $E_{ct}$ , and  $E_{disp}$  Computed Using the IMPT Procedure for the NaCl, Ar $_2$ , and (benzene) $_2$  Complexes, Taken As Prototype of Systems Presenting an Ionic or a van der Waals Bond<sup>a</sup>

complex	$E_{er}$	$E_{el}$	$E_{pol}$	$E_{ct}$	$E_{disp}$	$E_{int}$	$E_{MP2}$
NaCl	19.54	-141.21	-3.33	-4.23	-0.42	-129.66	-131.35
Ar $_2$	0.19	-0.05	<-0.01	<-0.01	-0.47	-0.33	-0.16
(C $_6$ H $_6$ ) $_2$	2.31	1.28	-0.16	-0.15	-3.59	-0.29	-0.26

<sup>a</sup> These calculations were done using the 6-31G(d,p) basis set, except Ar $_2$  that was computed using the aug-cc-pVDZ basis set to make a proper description of its attractive nature. The MP2/6-31G(d,p) interaction energy is also given, for comparison. All values are in kcal/mol. See text for definitions of the energy terms.

these radicals. Recent results on the phenalenyl dimer, **1**<sub>2</sub>, led to it being classified as a  $2e^-/12c$  bond<sup>3</sup> forced a revision of the rules to classify the electronic structure of long bonds, to be consistent with their nature, that is, defined on the basis of the dominant energetic component. This criterion is consistent with Pauling’s focus on bond energies as a criterion to define the presence of a bond.<sup>9</sup>

In the present work the nature of long bond between ion radical pairs and neutral radicals pairs is analyzed in deeper detail by identifying the dominant components of the interaction energy. The  $\pi$ -[TCNE] $_2^{2-}$  and the phenalenyl dimers are prototypes of long bonds in ion radical and neutral dimers, respectively. As a result of this study a clear differentiation between long bonds and covalent, ionic, or van der Waals bonds is computationally obtained. Finally, this enables a description of the electronic structure of the long bond, as  $me^-/nc$ , that is based on the dominant energetic component(s) in the interaction energy.

## Methodology

The analysis of the nature of a radical•••radical interaction can be done by identifying the strongest components in the interaction energy. When an AB dimer has only one  $2e^-$  intradimer bond, as for [TCNE] $^{\cdot-}$  and phenalenyl dimers, the properties of the interaction energy correspond to the properties of this intermolecular bond, in this case, the long, multicenter bond.

These components can be determined using intermolecular perturbation methods, as the intermolecular perturbation theory (IMPT) method.<sup>10</sup> However, there are no reported perturbative expressions that can be applied to open shell molecules. Therefore, we have to follow a qualitative approach in our estimates, although we have chosen to do it while preserving the philosophy of the perturbative treatments of the intermolecular interaction energy.

According to the IMPT method, the interaction energy ( $E_{int}$ ) of a closed shell AB generalized dimer can be written as the sum of the exchange-repulsion ( $E_{er}$ ), electrostatic ( $E_{el}$ ), polarization ( $E_{pol}$ ), charge-transfer, ( $E_{ct}$ ), and dispersion ( $E_{disp}$ ) components:

$$E_{int} = E_{er} + E_{el} + E_{pol} + E_{ct} + E_{disp} \quad (1)$$

The  $E_{er}$  component is associated to the repulsion that electrons feel when they occupy the same point of the space, in accord with the Pauli Exclusion Principle. It is always repulsive and can be qualitatively estimated as the exponential of the overlap integral of the wave functions of A and B.  $E_{el}$  is the electrostatic component from fragments which have the same charge and multipole moments

(7) Garcia-Yoldi, I.; Miller, J. S.; Novoa, J. J. *J. Chem. Phys. A* **2007**, *111*, 8020.

(8) Jung, Y.; Head-Gordon, M. *Phys. Chem. Chem. Phys.* **2004**, *6*, 2008. Garcia-Yoldi, I.; Mota, F.; Novoa, J. J. *J. Comput. Chem.* **2007**, *28*, 326.

(9) Pauling, L. *The Nature of the Chemical Bond*, 3rd ed.; Cornell University Press: Ithaca, NY, 1960; p 6. “We shall say that there is a chemical bond between two atoms or group of atoms in case that the forces acting between them are such as to lead to the formation of an aggregate with sufficient stability to make it convenient for the chemist to consider it as an independent molecular species”.

(10) Hayes, I. C.; Stone, A. J. *J. Mol. Phys.* **1984**, *53*, 83.

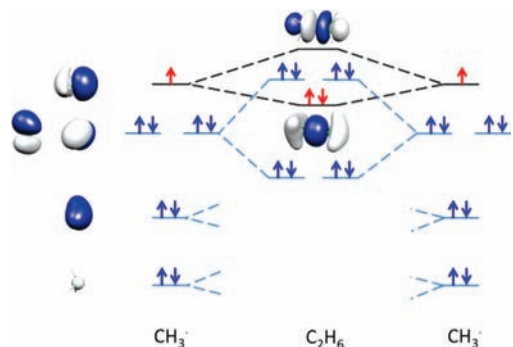


**Figure 2.** Simplified MO diagram for the formation of the C–C bond in  $C_2H_6$  in its closed-shell singlet ground state, by addition of two pyramidalized  $CH_3^\cdot$  radicals in their doublet ground state.

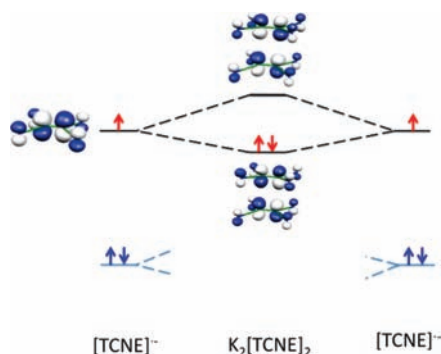


**Figure 3.** Simplified MO diagram associated to the formation of the long,  $2e^-/4c$  C–C bond for  $[TCNE]_2^{2-}$  in its closed-shell singlet ground state, by addition of two  $[TCNE]^\cdot$  radicals in their doublet ground state, and at the geometry of that the fragment has in the aggregate. The dimer orbitals were computed in a  $K_2[TCNE]_2$  aggregate by doing B3LYP/6-31+G(d) calculations.

when isolated, while  $E_{pol}$  is the polarization energy, which originates as result of the polarization of the A and B wave functions from their isolated form, due to the presence of the other fragment. Note that the sum of  $E_{el}$  and  $E_{pol}$  is the true electrostatic energy component. The charge transfer component,  $E_{ct}$  is the energy associated to the transfer of electronic charge from one fragment to the other. Finally, the dispersion component ( $E_{disp}$ ) is a nonclassical component arising from the instantaneous interactions of the electrons of A and B. In order to understand the magnitude of these components, Table 1 collects their value for a few representative dimers presenting ionic ( $Na^+ \cdots Cl^-$ ) or van der Waals ( $Ar_2$  and benzene  $\pi$ -dimer) bonds, where the A and B fragments are closed shell singlets.

When the interacting A and B fragments are both open shell, there is an extra component in the interaction energy whenever the orbitals of A and B are allowed to overlap. This is the case where  $A = B = [TCNE]^\cdot$  or phenalenyl $^\cdot$ , where the ground state is also a doublet and there is only one unpaired electron in each fragment. As result of the orbital overlap, bonding and antibonding combinations of the fragment orbitals are formed. The occupation of the AB orbitals according to the maximum occupancy principle allows the pairing the electrons that were unpaired in the A and B fragments. The energy gained by the AB complex in this pairing process is the bonding energetic component,  $E_{bond}$ , which adds to the other components in eq 1. Therefore, when open-shell fragments interact the main intermolecular energy takes the form:

$$E_{int} = E_{er} + E_{el} + E_{pol} + E_{ct} + E_{disp} + E_{bond} \quad (2)$$

Note, when  $A = B$ , as occurs for the dimers under consideration, the charge transfer term is expected to be very small. Previous

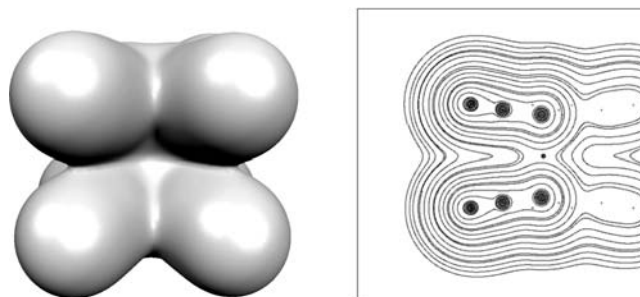


**Figure 4.** Representation of the B3LYP/6–31+G(d) electron density of  $[TCNE]_2^{2-}$  dimer. (Left) 3D isosurface of 0.003 atomic units; (Right) 2D cut of the electron density along the NC–C...C–CN plane (the position of the atoms is marked by the density accumulation), showing the presence of only one bond critical point (marked by a filled circle), linking the central C atoms (C...C bonding component).

studies<sup>10,11</sup> have also shown that the polarization term is usually 1 order of magnitude smaller than the electrostatic component, and also can be neglected in a qualitative analysis based on the dominant terms. The resulting expression for charged open-shell fragments is:

$$E_{int} = E_{er} + E_{el} + E_{disp} + E_{bond} \quad (3)$$

This equation is also valid in the absence of charge and dipole in both fragments, as in  $[TCNE]^\cdot$  and phenalenyl $^\cdot$  dimers, although  $E_{el}$  is expected to become less relevant (note that, as shown for the benzene  $\pi$ -dimers, Table 1, in the absence of charge and dipole the  $E_{el}$  component is not zero due to the presence of non-negligible dipole...quadrupole and quadrupole...quadrupole interactions).

The previous expressions can be applied to prototypical dimers presenting van der Waals, ionic and covalent bonds. For a typical van der Waals complex, for example,  $Ar_2$  or the  $\pi$ -dimer of benzene, the  $E_{bond}$  term is negligible, and thus the interaction energy reduces to:

$$E_{int} = E_{er} + E_{el} + E_{disp} \quad (4)$$

That for a typical ionic bond, e.g.  $Na^+ \cdots Cl^-$ , where two closed-shell charged fragments interact without pairing and the  $E_{disp}$  can be neglected, has the form:

$$E_{int} = E_{er} + E_{el} \quad (4a)$$

Finally, covalent bonds can be thought as dominated by the  $E_{bond}$  component, as the electrostatic and dispersion terms are numerically smaller. Consequently, it is possible to differentiate between long, covalent, ionic or van der Waals bonds by looking at the dominant energetic terms in the interaction energy,  $E_{int}$ .

As already mentioned, the weight of the energy components in eq 2 cannot be computed using the IMPT procedure,<sup>10</sup> or any similar procedure available in the literature. However, it is possible to qualitatively identify the dominant or the sum of the components by the following procedure:

(a) The Hartree–Fock method is known to give a proper qualitative estimate of the interaction energy of closed shell molecules from their open- or close-shell fragments, for both ionic or covalent complexes. In another words, it properly describes the sum of  $E_{er} + E_{el} + E_{pol} + E_{bond}$  terms for an AB complex (as ethane). It is, however, known to fail in reproducing the  $E_{disp}$  term properly, associated to the correlation energy,<sup>12</sup> whose estimation

(11) Novoa, J. J.; D’Oria, E. *Engineering of Crystalline Materials Properties*; Novoa, J. J., Braga, D., Addadi, L., Eds.; Springer: Dordrecht, 2008; pp 307–322.

(12) Szabo, A.; Ostlund, N. S. *Modern Quantum Chemistry*; Macmillan: New York, 1982.

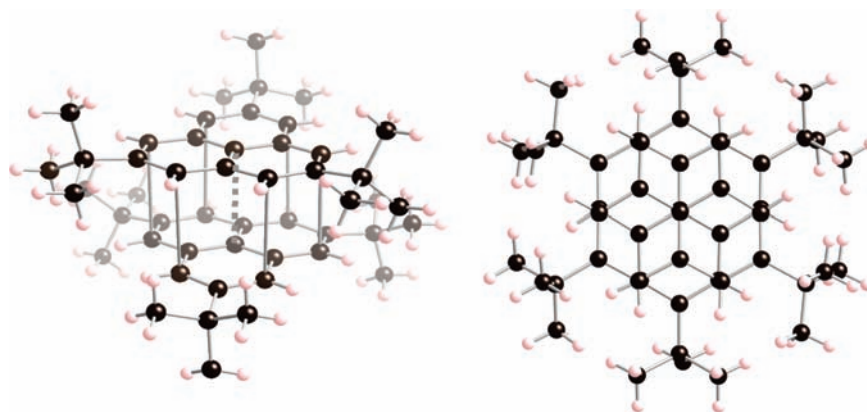


**Figure 5.** Lateral (left) and top (right) views of dimers of the neutral 2,5,8-tri-*t*-butylphenalenyl radical dimer.<sup>2</sup> The shortest C–C contacts between the monomers are indicated by solid lines (two contacts for each of these values: 2.296, 3.323, and 3.300 Å), with the only exception of the central C–C contact (3.201 Å), which is identified by a broken line.

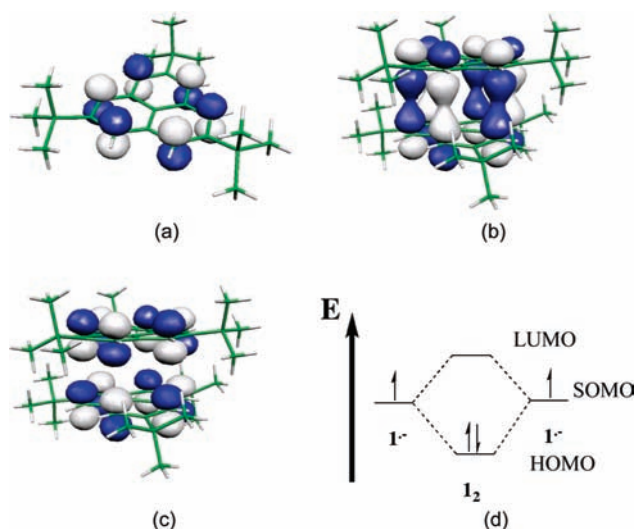


**Figure 6.** (a) SOMO of **1**; (b) HOMO of **1**<sub>2</sub>; (c) LUMO of **1**<sub>2</sub>; (d) qualitative MO diagram for the SOMO–SOMO overlap.

requires post Hartree–Fock methods (pHF) as the CASPT2<sup>13</sup> or the PP/MRMBPT2 methods.<sup>14</sup> Then,

$$E_{\text{disp}} = E_{\text{AB}}(\text{pHF}) - E_{\text{AB}}(\text{HF})$$

(b) The  $E_{\text{bond}}$  term that originates from pairing can be estimated as the difference between the closed-shell state of AB and the state of AB where the  $n$  unpaired electrons from the fragments are in their higher multiplicity state (in [TCNE]<sub>2</sub><sup>2-</sup> and phenalenyl dimers, a triplet state):

$$E_{\text{bond}} = E_{\text{AB}}(\text{CS}) - E_{\text{AB}}(\text{HS})$$

(c) The difference between  $E_{\text{int}}$  and  $E_{\text{bind}} + E_{\text{disp}}$  is equal to the sum of  $E_{\text{cr}} + E_{\text{cl}}$ . Its value should be similar for two molecules of the same charge and multipole moments placed at the same distance, a property that can serve as test of consistency of our estimations.

Note that this procedure is a general, quantitative estimate of their strengths, and does not make any assumption with respect to the nature or relative importance of any of the terms. The same applies to the AIM analysis, where the critical points are located

by searching for the computed total density without making any assumption on the origin of this density.

Unless otherwise stated, all calculations were done using the 6-31+G(d) basis set.<sup>15</sup> This basis set is of double- $\zeta$  plus polarization **quality** in the valence electrons, and has diffuse **functions** added for a proper description of the anions.<sup>16</sup> All energetic calculations, except those done using the CASSCF(2,2) or MRQDPT/CASSCF methods, were done using the appropriate options in Gaussian-03.<sup>17</sup> CASSCF and MCQDPT/CASSCF calculations were done using the GAMESS-07 suite of programs.<sup>18</sup>

## Results and Discussion

**Nature of the Long Bond between Ion Radicals.** The electronic structure of any long bond,  $ne^-/mc$ , was first defined<sup>1</sup> as follows: (1) the number of centers,  $m$ , in a long bond is established by looking at the number of atoms linked by ion radical/ion radical bond critical points, a value obtained from an atoms-in-molecules<sup>18</sup> (AIM) analysis of the electronic density, for example, for [TCNE]<sub>2</sub><sup>2-</sup> dimers in energetically stable K<sub>2</sub>[TCNE]<sub>2</sub> or similar neutral aggregates; and (2) the number of electrons,  $n$ , is the sum of the unpaired electrons in both radicals, and is typically 2, as occurs for [TCNE]<sub>2</sub><sup>2-</sup>.

It is now worth looking at the similarities and differences between the long bond found for  $\pi$ -[TCNE]<sub>2</sub><sup>2-</sup> and for a classical C–C covalent bond. The procedure chosen to find their differences is by looking at the differences in the  $E_{\text{int}}$  expression and in their MO diagram, summarized by indicating the value of  $n$  and  $m$  in the  $ne^-/mc$  classification. The classical C–C covalent bond in ethane can be taken as a simple prototype (Figure 2, where we visualize the formation from their pyramidalized fragments, to discount the energy to distort each CH<sub>3</sub><sup>•</sup> radical from its most stable coplanar form). The C–C bond in ethane can be viewed as the result of pairing the unpaired electron located in each CH<sub>3</sub><sup>•</sup> radical. The SOMO–SOMO pairing ( $E_{\text{bond}}$ ) is the main energetic component in the intermolecular interaction energy of the CH<sub>3</sub><sup>•</sup> + CH<sub>3</sub><sup>•</sup> → C<sub>2</sub>H<sub>6</sub> process.

(13) Roos, B. O.; Andersson, K.; Fulscher, M. K.; Malmqvist, P. A.; Serrano-Andres, L.; Pierloot, K.; Merchan, M. *Adv. Chem. Phys.* **1996**, *93*, 219.

(14) Nakano, H.; Nakayama, K.; Hirao, K.; Dupuis, M. *J. Chem. Phys.* **1997**, *106*, 4912.

(15) A basis set built by adding diffuse functions to the 6-31G(d) basis set. The later is described in: Ditchfield, R.; Hehre, W. J.; Pople, J. A. *J. Chem. Phys.* **1971**, *54*, 724.

(16) Clark, T.; Chandrasekhar, J.; Spitznagel, G. W.; Scheleyer, P.v.R. *J. Comp. Chem.*, **1983**, *4*, 294.

(17) Gaussian-03, Revision-C.02, Frisch, M. J., et al; Gaussian, Inc., Wallingford CT, 2004.

(18) Schmidt, M. W.; Baldridge, K. K.; Boatz, J. A.; Elbert, S. T.; Gordon, M. S.; Jensen, J. H.; Koseki, S.; Matsunaga, N.; Nguyen, K. A.; Su, S. J.; Windus, T. L.; Dupuis, M.; Montgomery, J. A. *J. Comput. Chem.* **1993**, *14*, 1347.

**Table 2.** Computed  $E_{\text{int}}$  for the Singlet and Triplet States of  $[\text{TCNE}]_2^{2-}$  Using the Indicated Methods and the 6-31+G(d) Basis Set

method	$[\text{TCNE}]_2^{2-}$ singlet, kcal/mol	$[\text{TCNE}]_2^{2-}$ triplet, kcal/mol
CAS(2,2)/ROHF <sup>a</sup>	67.9	80.9
RB3LYP/UB3LYP <sup>b</sup>	63.4	75.1
MP2/MRMBPT2 <sup>c</sup>	40.0	55.9

<sup>a</sup> CASSCF(2,2) method was used for the singlet state, while the ROHF method was used for the triplet state. <sup>b</sup> RB3LYP functional was used for the singlet state, while the UB3LYP functional was used for triplet states. <sup>c</sup> ROMP2 method was used for triplet state, while the MRMBPT2 method on a CASSCF(2,2) reference wave function was used for the singlet state.

**Table 3.**  $E_{\text{int}}$ ,  $E_{\text{bond}}$ ,  $E_{\text{disp}}$ , and  $E_{\text{er}}$  for  $[\text{TCNE}]_2^{2-}$ <sup>a</sup>

dimer	$E_{\text{int}}$ , kcal/mol	$E_{\text{bond}}$ , kcal/mol	$E_{\text{disp}}$ , kcal/mol	$E_{\text{er}} + E_{\text{el}}$ , kcal/mol
$\text{I}_2$ singlet state	40.0	-15.9	-27.7	83.6
$\text{I}_2$ triplet state	55.9	0.0 <sup>b</sup>	-25.0	80.9

<sup>a</sup> They have been computed using the data in Table 1 using the procedures indicated in the text. <sup>b</sup> This component does not exist in this state

The qualitative MO diagram of Figure 2 pictorially describes the main changes produced in the electronic structure of the two  $\text{CH}_3^\cdot$  radicals (in their doublet ground state) when they interact to form a  $\text{C}_2\text{H}_6$ , in its closed-shell singlet ground state. The SOMO of one  $\text{CH}_3^\cdot$  radical overlaps with the same orbital in the other radical, thus inducing the formation of a bonding and antibonding  $\text{C}_2\text{H}_6$  orbital (only the combinations originating from the highest three fragment orbitals are explicitly shown). Doubly occupied fragment orbitals result in doubly occupied bonding and antibonding orbitals, and a very small gain in energy. The most important gain is obtained from the SOMO overlap, as the bonding combination gets two electrons while the antibonding gets none. Therefore, from an electronic and energetic point of view, the new C–C bond is primarily a result of the overlap of the two unpaired  $\text{CH}_3^\cdot$  electrons in the SOMO orbitals, which are mostly located on the two carbon centers. Consequently, it seems appropriate to represent this bond as a  $2e^-/2c$  bond; the most common type of bond invoked in chemistry. This result is consistent with those of an AIM analysis.

The MO diagram obtained when two  $[\text{TCNE}]^\cdot$  doublets interact to form  $[\text{TCNE}]_2^{2-}$  (Figure 3) is similar to that in Figure 2. Note that the of these orbitals have been computed for an  $\text{K}_2[\text{TCNE}]_2$  aggregate, where two electrons are located in each  $[\text{TCNE}]^\cdot$ . In a natural form, they are located in the HOMO, whose orbital energy is negative (thus guaranteeing that they will not spontaneously ionize). Hence, it is tempting to associate the properties of long bonds solely to the SOMO–SOMO overlap,  $m$  thus being the number of atom-pairs that show in-phase orbital lobe overlapping combinations in the SOMO + SOMO combination. However, this association can result in inconsistent conclusions. For instance, the SOMO + SOMO combination in the  $[\text{TCNE}]_2^{2-}$  dimer (Figures 1 and 3) has six in-phase overlapping lobes between the SOMO fragments (those connecting the central C atoms, but also those connecting all of the N atoms in one fragment with the nearest ones of the second fragment). Therefore, the long bond in the  $[\text{TCNE}]_2^{2-}$  dimer would be a  $2e^-/12c$  bond.

The presence of  $\text{N}\cdots\text{N}$  bonding components for  $[\text{TCNE}]_2^{2-}$  is inconsistent with the bending away that is observed in the CN groups, which is in accord with the CN groups avoiding each other. This bending is understood by realizing that in

$[\text{TCNE}]_2^{2-}$  the electrostatic component is stronger than the component that originates from the SOMO–SOMO overlap,  $E_{\text{bond}}^{1,3,8,6,7}$ .  $E_{\text{elec}}$  is minimized when the CN groups, which concentrate a large part of the net negative charge in each fragment, bends away of each other. The cation $\cdots$ anion radical interaction is also maximized when the CN bend away, as regions of negative charge get closer to the cations. Therefore, *long bonds cannot be associated solely to the SOMO–SOMO overlap, and the dominant energetic components must be identified.*

An AIM analysis automatically takes into account the presence of all relevant energetic components to the bond. Note here that not all components are properly accounted in all methods (for instance, by definition, dispersion is not accounted in Hartree–Fock calculations) and thus an AIM analysis should be done on wave functions obtained by proper methods.<sup>19</sup> For  $[\text{TCNE}]_2^{2-}$  the  $\text{N}\cdots\text{N}$  interaction is not a bonding component in Hartree–Fock, B3LYP or CASSCF(2,2) wave functions, as  $\text{N}\cdots\text{N}$  has no bond critical point for the  $[\text{TCNE}]_2^{2-}$  density computed using any of these methods (no AIM analysis was done on the CASSCF(2,2)/MRMP2 wave function because it is a perturbative calculation on a CASSCF(2,2) reference wave function). The absence of these  $\text{N}\cdots\text{N}$  bond critical points is graphically demonstrated when plotting the electron density of this dimer, Figure 4: two  $\text{C}\cdots\text{C}$  bond critical point exist, which links the central C atoms (its existence is visually associated to the funnel that connects these two atoms in the right part of Figure 4). Hence, the shape of the electronic distribution reflects the effect of all energetic components.<sup>19</sup>

Note that analyzing the bond by looking at the sum of all its main energetic components is consistent with the general philosophy behind the landmark work of Pauling on the nature of bonds. Besides defining bonds,<sup>9</sup> he also noted that bond energies should be chosen in such a way that their sum over all of the bonds should be equal to the enthalpy of formation from its constituent atoms in their normal states.<sup>20</sup> That is, he focused on bond energies, and the dominant bonds components are a good representation of total bond energies.

Finally, in order to evaluate if the previous results are consistent with the dominant components of the interaction energy, the values of  $E_{\text{er}} + E_{\text{el}}$ ,  $E_{\text{disp}}$ , and  $E_{\text{bond}}$  need to be estimated using the procedure described in the Methodology. A quantitative evaluation of the relative contributions of the  $E_{\text{disp}}$ ,  $E_{\text{bond}}$ , and  $E_{\text{er}} + E_{\text{el}}$  components in the interaction energy of  $[\text{TCNE}]_2^{2-}$  can be done as follows:

(a)  $E_{\text{bond}}$  in the singlet state of  $[\text{TCNE}]_2^{2-}$  can be approximated as the energy difference between the closed-shell singlet and its associated triplet state (Table 2). Due to the multiconfigurational nature of the closed-shell singlet (manifested in the 1.63 and 0.37 occupation of the two active orbitals when doing CASSCF(2,2) calculations,<sup>20</sup> which are the HOMO and LUMO of Figure 4), the energy of the singlet state is better taken as

(19) Bader, R. F. W. *Atoms in Molecules. A Quantum Theory*, Clarendon Press, Oxford, 1990.

(20) Pauling, L. *The Nature of the Chemical Bond*, 3rd ed.; Cornell University Press: Ithaca, NY, 1960; p 622. "In Chapter 3 and other chapters of this book much use is made of bond-energy values. These values are chosen in such a way that their sum over all of the bonds of a molecule which can be satisfactorily represented by a single valence-bond structure is equal to the enthalpy of formation of the molecule from its constituent atoms in their normal states". The statement was done for molecules that can be properly represented by a single valence bond structure, that is, that have no resonant structures of similar energies.

the CASSCF(2,2) value,<sup>21</sup> while that for the triplet state can be taken from a Restricted Open Hartree–Fock calculation for technical reasons, which is identical to that obtained at the CASSCF(2,2) level. The value this obtained is  $-13.0$  kcal/mol (the minus sign indicates that it is an attractive energetic component). Note the similarity between this value and that obtained by the  $E_{\text{RB3LYP}}(\text{singlet}) - E_{\text{UB3LYP}}(\text{triplet})$  subtraction values in Table 2,  $-11.7$  kcal/mol.

(b)  $E_{\text{disp}}$  in the singlet state of  $[\text{TCNE}]_2^{2-}$  can be calculated by subtracting the CASSCF(2,2) interaction energy for the singlet from the MRMBPT2 energy for the same state, Table 2, and is  $-27.9$  kcal/mol. When the same subtraction is done for the triplet state the difference becomes  $-25.0$  kcal/mol. The similarity of these two values indicates the consistency of this estimate.

(c) The sum of  $E_{\text{er}} + E_{\text{el}}$ , can be estimated by subtracting  $E_{\text{int}}$  from  $E_{\text{bind}} + E_{\text{disp}}$ . This results in  $83.6$  kcal/mol for the singlet state, and  $80.9$  kcal/mol for the triplet state. As previously shown,<sup>6</sup> the repulsion nature of these two values is mostly caused by the electrostatic component.

These estimates show that  $E_{\text{bond}} < E_{\text{disp}}$ , although both are attractive, and that their sum is smaller than  $E_{\text{er}} + E_{\text{el}}$ , justifying the net repulsive character of  $E_{\text{int}}$  in  $[\text{TCNE}]_2^{2-}$ . The dominant attractive component is the dispersion component ( $-27.7$  kcal/mol) that is about twice the bonding component ( $-15.9$  kcal/mol). These results further confirm the consistency of the  $2e^-/4c$  classification of the electronic structure in  $[\text{TCNE}]_2^{2-}$  (Table 3).<sup>23</sup>

**Nature of the Long Bond between Neutral Radicals.** In addition to the intradimer dianion and dication long bonding, the intradimer long bonding in neutral radical dimers can be evaluated. The phenalenyl dimer,  $\mathbf{1}_2$ , is taken as the prototype of the later because  $\mathbf{1}_2$  is the best characterized (experimentally and theoretically) example of a neutral radical dimer presenting a long bond.<sup>2,3</sup> EPR and UV spectra studies in the solid state and in solution indicate that  $\mathbf{1}_2$  has a diamagnetic ground state.<sup>2,3</sup> In the solid, this diamagnetism is consistent with a strong antiferromagnetic interaction observed within the dimer<sup>2</sup> ( $2J/k_B = -2000$  K). In solution, this diamagnetism is consistent with the disappearance of the excited state triplet EPR signal as the temperature is reduced, a process accompanied with a simultaneous growth of an absorption at  $589$  nm.<sup>3</sup> The structure of  $\mathbf{1}_2$  (Figure 5) has  $D_{3d}$  symmetry, and the shortest interfragment C–C contact ( $3.201$  Å) involves the two central eclipsed C atoms.<sup>2</sup> In addition, there are six eclipsed interfragment C–C contacts  $< 3.330$  Å that are less than the sum of the van der Waals radii. Thus, if subvan der Waals contacts are indicative of a van der Waals bond, the  $2e^-$  intradimer bonding for  $\mathbf{1}_2$

**Table 4.** Computed  $E_{\text{int}}$  for the Singlet and Triplet States of the  $\mathbf{1}_2$  and  $\mathbf{1}_2(\text{N}2)$  Dimers Using the Indicated Methods and the 6-31+G(d) Basis Set

method	$\mathbf{1}_2$ singlet, kcal/mol	$\mathbf{1}_2$ triplet, kcal/mol	$\mathbf{1}_2(\text{N}2)$ singlet, kcal/mol
CAS(2,2)/ROHF/RHF <sup>a</sup>	1.1	14.0	16.3
RB3LYP/UB3LYP <sup>b</sup>	0.5	8.2	8.7
MP2/MRMBPT2 <sup>c</sup>	$-26.0$	$-17.7$	$-16.2$

<sup>a</sup> CASSCF(2,2) method was used for the  $\mathbf{1}_2$  singlet state, while the ROHF method was used for the  $\mathbf{1}_2$  triplet state, and the RHF method was used for the  $\mathbf{1}_2(\text{N}2)$  singlet state. <sup>b</sup> RB3LYP functional was used for the singlet state, while the UB3LYP functional was used for triplet states. <sup>c</sup> MP2 method was used for  $\mathbf{1}_2$  triplet state and  $\mathbf{1}_2(\text{N}2)$  singlet state, while the MRMBPT2 method using a CASSCF(2,2) reference wave function was used for the  $\mathbf{1}_2$  singlet state.

**Table 5.**  $E_{\text{int}}$ ,  $E_{\text{bond}}$ ,  $E_{\text{disp}}$ , and  $E_{\text{er}}$  for  $\mathbf{1}_2$  and  $\mathbf{1}_2(\text{N}2)$ <sup>a</sup>

Dimer	$E_{\text{int}}$ , kcal/mol	$E_{\text{bond}}$ , kcal/mol	$E_{\text{disp}}$ , kcal/mol	$E_{\text{er}} + E_{\text{el}}$ , kcal/mol
$\mathbf{1}_2$ singlet state	$-26.0$	$-12.9$	$-31.7$	18.5
$\mathbf{1}_2$ triplet state	$-17.7$	$0.0^b$	$-31.7$	14.0
$\mathbf{1}_2(\text{N}2)$ singlet state	$-16.2$	$0.0^b$	$-32.5$	16.3

<sup>a</sup> Components have been computed using the data in Table 1 using the procedures indicated in the text. <sup>b</sup> This component does not exist in this state

should be a long  $2e^-/4c$  bond. Finally, from solution studies it is known that the enthalpy of dimerization is  $-9.5$  kcal/mol,<sup>3</sup> a typical value for van der Waals dimers.<sup>24</sup>

The energetic considerations applied above for ion radical dimers do not explain the existence of multicenter long C–C bonding in  $\mathbf{1}_2$ . The absence of net charge and the  $D_{3h}$  symmetry of the interacting radicals (which results in a negligible dipole moment) suggest that the electrostatic energetic component should be very small.  $E_{\text{ct}}$  is also expected to be negligible, as both fragments are identical. Therefore, the stability of  $\mathbf{1}_2$  should arise from the  $E_{\text{bond}}$  and  $E_{\text{disp}}$  components, complemented with a smaller  $E_{\text{el}}$  component. This conclusion is in good agreements with previous estimates on the nature of this bond.<sup>3</sup> As in all dimers, the repulsive  $E_{\text{er}}$  component exceeds the sum of all other components at very short distances.<sup>10,25</sup> However, its strength decreases exponentially with the distance between the interacting fragments, and at large enough distances, the  $E_{\text{bond}} + E_{\text{disp}} > E_{\text{er}}$ , allowing the existence of a minimum in the radical–radical potential energy curve, as reported.<sup>3</sup> Thus,  $\mathbf{1}_2$  is stable “per se” against its dissociation, which is at variance for  $[\text{TCNE}]_2^{2-}$ . This stability is in accord to that found in closed-shell dimers, for example, the benzene  $\pi$ -dimers, a typical van der Waals dimer. Therefore, the long bond in  $\mathbf{1}_2$  can be considered as arising from van der Waals plus bonding interactions.

The covalent-like properties of the  $\mathbf{1}_2$  dimers were attributed<sup>3</sup> to the overlap of the SOMOs of the fragments at the equilibrium distance. This overlap generates a doubly occupied in-phase orbital and an empty out-of-phase orbital, Figure 6.<sup>3,26</sup> Thus, the qualitative MO diagram in  $\mathbf{1}_2$  is typical of conventional covalent bonds and explains the covalent-like properties of  $\mathbf{1}_2$

- (21) In CASSCF(2,2) calculations, a pure closed-shell singlet would present an occupation of the two active orbitals of 2.0 and 0.0, while a pure open-shell singlet would have an occupation of 1.0 and 1.0. An occupation of 1.63 and 0.37 indicates that the ground state singlet is mostly closed-shell in nature, but has a non-negligible contribution of the open-shell singlet.
- (22) Previous calculations described in reference<sup>3</sup> have shown that the closed-shell singlet of  $\mathbf{1}_2$  is a mixture of the HOMO<sup>2</sup>LUMO<sup>0</sup> and HOMO<sup>1</sup>LUMO<sup>1</sup> singlet configurations, whose description requires at least a CASSCF(2,2) wavefunction.
- (23) The description made up to now of the long bond in  $[\text{TCNE}]_2^{2-}$  uses the MO formalism. It is possible that an equivalent description using the valence bond formalism can also be developed. In this case, the long bond in  $[\text{TCNE}]_2^{2-}$  involves three electrons sitting on the two C=C atoms of each fragment. The bond is formed between the unpaired electrons, and there are two equivalent resonant forms: one where the two bonded atoms are the left ones, and one where the two bonded atoms are the right ones (in both forms, the other atoms hold two electrons each).

- (24) Israelachvili, J. *Intermolecular and Surface Forces*, 2nd ed.; Academic Press: Amsterdam, 1991. Maitland, G. C.; Rigby, M.; Smith, E. B.; Wakeham, W. *Intermolecular forces: Their origin and determination*; Clarendon Press: Oxford, 1981.
- (25) The  $E_{\text{er}}$  term is dominant at very short distances, and all intermolecular interactions are repulsive at very short distances. See, for instance, Figure 3 in ref 10.
- (26) Fukui, K.; Sato, K.; Shiomi, D.; Takui, T.; Itoh, K.; Gotoh, K.; Kubo, T.; Yamamoto, K.; Nakasuji, K.; Naito, A. *Syn. Met* **1999**, *103*, 2257. Takano, Y.; Taniguchi, T.; Isobe, H.; Kubo, T.; Morita, Y.; Yamamoto, K.; Nakasuji, K.; Takui, T.; Yamaguchi, K. *J. Am. Chem. Soc.* **2002**, *124*, 11122.

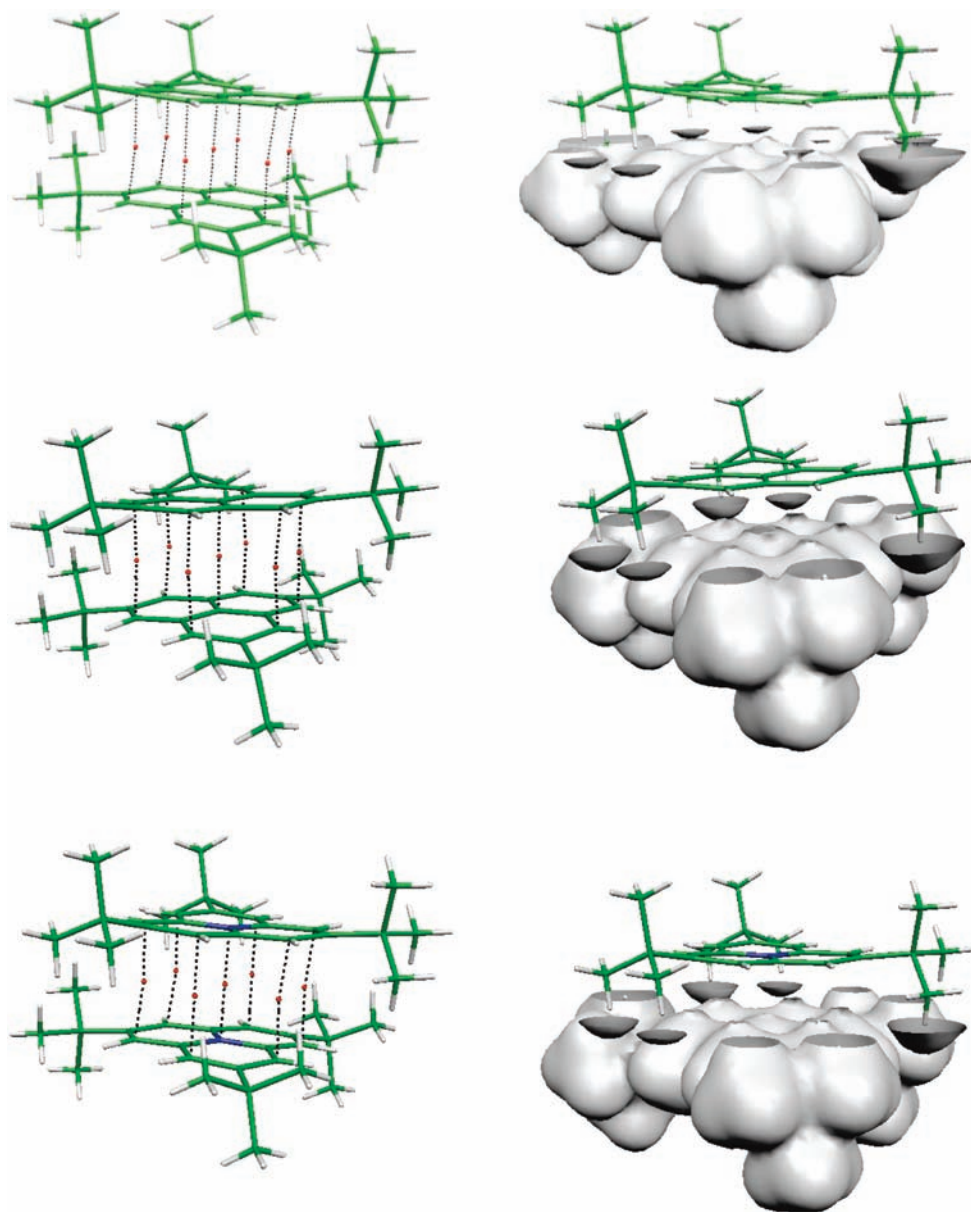


**Figure 7.** Location of the bond critical points found in the closed-shell singlet state of  $\mathbf{1}_2$  (top-left), and shape of the B3LYP/6-31+G(d) electron density isosurface of 0.002 atomic units cut along the plane of the bond-critical points (top-right); equivalent representations for the triplet state of  $\mathbf{1}_2$  (middle), and closed-shell singlet of  $\mathbf{1}_2(\text{N}2)$  (bottom). Each of the funnels seen in the density isosurface indicates the presence of a bond critical point.

(i.e., diamagnetic ground state, origin of the UV spectra). Upon only considering the bonding component ( $E_{\text{bond}}$ ), the long bond in  $\mathbf{1}_2$  was classified as a  $2e^-/12c$  C–C bond<sup>3</sup> on the basis of the number of in-phase combinations that the fragments SOMO have in the dimer HOMO, as neither the HOMO nor the LUMO of  $\mathbf{1}_2$  has a contribution on these central C atoms, despite the central C–C distance being the shortest, because the SOMOs have no component on the central C atoms, Figure 6.<sup>27</sup>

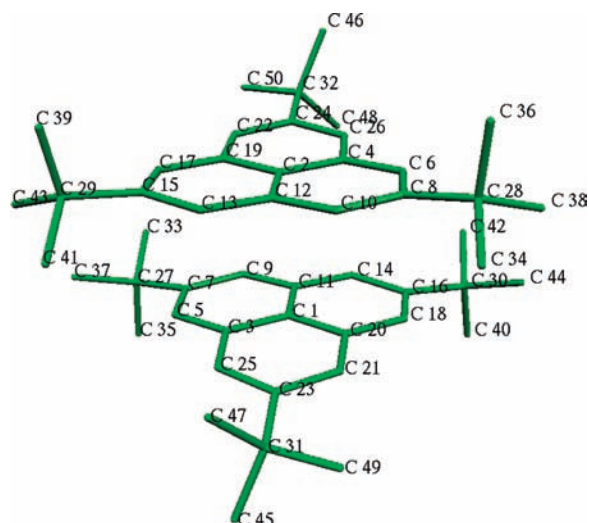
To identify the dominant energy component for  $E_{\text{int}}$  the energies of  $E_{\text{cr}} + E_{\text{el}}$ ,  $E_{\text{disp}}$ , and  $E_{\text{bond}}$  need to be estimated, using the procedure described in the Methodology. Hartree–Fock and

B3LYP calculations<sup>3</sup> were used to determine the stability of  $\mathbf{1}_2$ , which is energetically unstable with respect to dissociation into two phenalenyl fragments. However,  $\mathbf{1}_2$  was found to be energetically stable by PP/MRMBPT2 calculations,<sup>28</sup> with the calculated stability ( $-26.0$  kcal/mol, at the experimental inter-fragment distance) in the range of the experimental interaction energy in solution ( $-9.5$  kcal/mol).<sup>3,29</sup> Therefore, the dispersion component, which is not accounted at all in Hartree–Fock calculations, and improperly accounted in B3LYP calculations, is essential for the stability of the dimer, as occurs for van der Waals dimers. Furthermore, the equilibrium distance and optimum stability of  $\mathbf{1}_2$  are typical of pure van der Waals

(27) This description is based on a molecular orbital formalism. It is also possible an equivalent valence bond description of the long bond in phenalenyl dimers, where the most evident resonant form is that where the unpaired electron is placed in the central C atom in both fragments. The two unpaired electrons from each fragment form then a C–C bond. There are more resonant forms, which delocalize the unpaired electron over all peripheral C atoms (see refs 2 and 3).

(28) Nakano, H. *J. Chem. Phys.* **1993**, *99*, 7983.

(29) Note that the computed interaction energy of a phenalenyl dimer and the experimental DH in solution necessarily differ, due to the phenalenyl–solvent interactions in solution and to the reorganization energy of the solvent when the pairs are formed.

**Table 6.** Electron Density and Laplacian at the Bond Critical Point (Atomic Units) of the Bond-Critical Points Found in the Closed-Shell Singlet States of  $\mathbf{1}_2$  and  $\mathbf{1}_2(\text{N}_2)$ , and the Singlet State of  $\mathbf{1}_2^a$ 

$\mathbf{1}_2$ singlet			$\mathbf{1}_2$ triplet			$\mathbf{1}_2(\text{N}_2)$		
bonded atoms	electron density	Laplacian	bonded atoms	electron density	Laplacian	bonded atoms	electron density	Laplacian
C1–C2	0.004	0.014	C1–C2	0.007	0.041	N1–N2	0.009	0.023
C10–C21	0.003	0.011	C10–C21	0.005	0.018	C10–C21	0.005	0.018
C13–C25	0.004	0.014	C13–C25	0.005	0.018	C13–C25	0.005	0.018
C14–C26	0.004	0.014	C14–C26	0.005	0.018	C14–C26	0.005	0.017
C5–C17	0.003	0.012	C5–C17	0.006	0.018	C5–C17	0.006	0.018
C6–C18	0.003	0.012	C6–C18	0.006	0.018	C6–C18	0.006	0.018
C9–C22	0.004	0.011	C9–C22	0.005	0.018	C9–C22	0.005	0.018

<sup>a</sup>  $\mathbf{1}_2$  and  $\mathbf{1}_2(\text{N}_2)$  properties were obtained using the CASSCF(2,2) and ROMP2 wavefunction, respectively. The 6-31+G(d) basis set was used in these calculations.

dimers.<sup>30</sup> Hence,  $\mathbf{1}_2$  has a dispersion-dominated interaction energy, and the bond is best described as a  $2e^-/14c$  long bond, rather than the  $2e^-/12c$ , which is suggested only on the basis of the  $E_{\text{bond}}$  contribution.

A quantitative evaluation of the relative contributions of the  $E_{\text{disp}}$ ,  $E_{\text{bond}}$ , and  $E_{\text{er}} + E_{\text{el}}$  components in the interaction energy of  $\mathbf{1}_2$  is done by the aforementioned methods:

(a)  $E_{\text{bond}}$  in the singlet state of  $\mathbf{1}_2$  can be approximated as the energy difference between the closed-shell singlet and its associated triplet state, which is  $-12.9$  kcal/mol (the minus sign indicates that it is an attractive energetic component) (Table 4). As for  $[\text{TCNE}]_2^{2-}$ , due to the multiconfigurational nature of the closed-shell singlet (manifested in the 1.72 and 0.28 occupation of the two active orbitals when doing CASSCF(2,2) calculations,<sup>31</sup> which are the HOMO and LUMO of Figure 4), the energy of the singlet state is better taken as the CASSCF(2,2) value,<sup>32</sup> while that for the triplet state can be taken from a Restricted Open Hartree–Fock calculation for technical reasons, which is identical to that obtained at the CASSCF(2,2) level. The value of  $E_{\text{bond}}$  in  $\mathbf{1}_2$  is very close to that obtained for

$[\text{TCNE}]_2^{2-}$  ( $-13.0$  kcal/mol), in good agreement with the similar distance at which the fragments in these two dimers are located. Note that this value is similar to that obtained by subtracting  $E_{\text{RB3LYP}}(\text{singlet}) - E_{\text{UB3LYP}}(\text{triplet})$ ,  $-7.7$  kcal/mol.

(b)  $E_{\text{disp}}$  in the singlet state of  $\mathbf{1}_2$  can be calculated by subtracting the CASSCF(2,2) interaction energy for the singlet from the MRMBPT2 energy for the same state, and is  $-27.1$  kcal/mol. This is similar to the  $E_{\text{disp}}$  computed for the triplet state of  $\mathbf{1}_2$  ( $-31.7$  kcal/mol, computed by subtracting the Hartree–Fock and MP2 interaction energy for this state). Note also the similarity with the value of  $E_{\text{disp}}$  in  $[\text{TCNE}]_2^{2-}$  ( $-27.7$  and  $-25.0$  kcal/mol for the singlet and triplet state, respectively, Table 3). The values of  $E_{\text{disp}}$  in  $\mathbf{1}_2$  can also be compared to those obtained for a hypothetical  $\mathbf{1}_2$  analogue where the central C atom in each phenalenyl is substituted by a N atom,  $\mathbf{1}_2(\text{N}_2)$ , a closed-shell, pure van der Waals dimer with a structure very similar to that for  $\mathbf{1}_2$ . As is usual in van der Waals dimers,  $\mathbf{1}_2(\text{N}_2)$  is energetically unstable at the Hartree–Fock level by 16.3 kcal/mol, but becomes stable ( $-16.2$  kcal/mol) when the interaction energy is computed at the MP2 level, a method that accounts for the majority of the dispersion component (the difference between the Hartree–Fock and MP2 total energies is the correlation energy, which in this dimer is basically associated to the dispersion component). Therefore,  $E_{\text{disp}}$  for  $\mathbf{1}_2(\text{N}_2)$  (Table 5, computed as the difference between the RHF and MP2 interaction energies) is  $-32.5$  kcal/mol; a result that is close to that computed for the singlet and triplet state of  $\mathbf{1}_2$  ( $-27.1$  and  $-31.7$  kcal/mol, respectively, Table 3),

(c) The sum of  $E_{\text{er}} + E_{\text{el}}$ , can be estimated by subtracting  $E_{\text{int}}$  from  $E_{\text{bind}} + E_{\text{disp}}$ . Note that  $E_{\text{er}} + E_{\text{el}}$  thus obtained is similar for both  $\mathbf{1}_2$  and  $\mathbf{1}_2(\text{N}_2)$ , as it corresponds to the small changes

(30) The BSSE corrected MP2/6-31+G(d) interaction energy for  $\text{Ar}_2$ ,  $(\text{CO}_2)_2$  and  $p$ -(benzene)<sub>2</sub> dimers at the minimum of their interaction energy curves are  $-0.16$ ,  $-1.0$  and  $-1.8$  kcal/mol, being the associated equilibrium distances 3.842, 3.058 and 3.800 Å, respectively (see ref 10).

(31) As justified in ref 16, an occupation of 1.72 and 0.28 in CASSCF(2,2) calculations indicates that the ground state singlet is mostly closed-shell in nature, but with a non-negligible contribution of the open-shell singlet.

(32) Previous calculations described in reference<sup>3</sup> have shown that the closed-shell singlet of  $\mathbf{1}_2$  is a mixture of the HOMO<sup>0</sup>LUMO<sup>0</sup> and HOMO<sup>1</sup>LUMO<sup>1</sup> singlet configurations, whose description requires at least a CASSCF(2,2) wavefunction.



in the electronic states of these two molecules, which have an identical geometry.

$E_{\text{bond}} < E_{\text{disp}}$ , Table 5, is in accord with the  $E_{\text{bond}}$  being insufficient to stabilize the dimer. Furthermore,  $E_{\text{disp}}$  for  $\mathbf{1}_2$  is 2.46 times  $E_{\text{bond}}$ , and the nature of  $\mathbf{1}_2$  is closer to a van der Waals than to a covalent dimer.

The similarity to a van der Waals dimer for  $\mathbf{1}_2$  obtained from the above qualitative estimation can also be provided by an AIM analysis of the bonding in  $\mathbf{1}_2$  (Figure 7, top and Table 3) where the results for  $\mathbf{1}_2$  were compared with that of the pure  $\mathbf{1}_2(\text{N}_2)$  van der Waals dimer (Figure 7, bottom, and Table 6). Seven  $\mathbf{1}\cdots\mathbf{1}$  bond critical points were found for both  $\mathbf{1}_2$  and  $\mathbf{1}_2(\text{N}_2)$  (Figure 7), the six that have orbital overlap in the HOMO of  $\mathbf{1}_2$  (Figure 4b), and the central  $\text{C}\cdots\text{C}$  bond of  $\mathbf{1}_2$ , which in  $\mathbf{1}_2(\text{N}_2)$  is replaced by a central  $\text{N}\cdots\text{N}$  interaction. Furthermore, the electron density and the Laplacian at the bond critical point<sup>19</sup> is very similar for all of the bond critical points calculated for  $\mathbf{1}_2(\text{N}_2)$  and  $\mathbf{1}_2$ , (Table 6). Therefore,  $\mathbf{1}_2$  exhibits bond critical points similar to a pure van der Waals dimer. Furthermore, the number of the  $\mathbf{1}\cdots\mathbf{1}$  bond critical points in the closed-shell singlet and triplet state of  $\mathbf{1}_2$  are identical, and their electron density and Laplacian very similar, Table 6. Note that the triplet state of  $\mathbf{1}_2$  is a pure van der Waals dimer ( $E_{\text{bond}}$  is zero, as there is no pairing). The similarity in the electron density of the closed-shell singlet and triplet states of  $\mathbf{1}_2$  is only possible if  $E_{\text{bond}}$  for the singlet is small. All these results suggest that the long bond in the singlet is best described as a  $2e^-/14c$  bond.<sup>33</sup>

## Conclusion

In accord with Pauling's focus on total bond energies,<sup>9</sup> and not only on one of its components, the properties of the long, multicenter bond in the 2,5,8-tri-*t*-butylphenalenyl dimer,  $\mathbf{1}_2$ , are investigated in detail by comparing the computed energy components its electronic structure with (a) that for  $[\text{TCNE}]_2^{2-}$ , a prototype of long bond between ion radicals, and (b) those of a dimer where the central C atom in both phenalenyl fragments

are substituted by a N atom,  $\mathbf{1}_2(\text{N}_2)$ , a pure van der Waals dimer where both fragments are closed-shell singlets and thus the SOMO–SOMO bonding component is zero. The dispersion component of the interaction energy in  $\mathbf{1}_2$  is 2.46 times stronger than the bonding component. Therefore, the interaction energy of  $\mathbf{1}_2$  is very similar to that for a pure van der Waals dimer. The bonding component in  $\mathbf{1}_2$  is similar ( $-12.9$  kcal/mol) to that found in  $[\text{TCNE}]_2^{2-}$  ( $-13.0$  kcal/mol). Finally, an AIM analysis of the electron density for the closed-shell singlet state of  $\mathbf{1}_2$  and  $\mathbf{1}_2(\text{N}_2)$  reveals seven bond-critical points with nearly the same characteristic properties. Hence, the multicenter bonding in  $\mathbf{1}_2$  has a dominant  $2e^-/14c$  character. The covalent-like properties in  $\mathbf{1}_2$  result from the dominant dispersion component that enable the fragments to approach each other so that their SOMOs overlap and produce a qualitative MO diagram identical to that found in conventional covalent bonds. The rules followed to assign the number of electrons and centers in long bonds in  $[\text{TCNE}]_2^{2-}$  are also revised and found consistent with its previous  $2e^-/4c$  character. Note that although the intradimer bonds in  $[\text{TCNE}]_2^{2-}$  and phenalenyl dimers are both  $2e^-$ , as are all long bonds studied to date,<sup>1–8</sup> it is not necessary for all long bonds have to involve two electrons. It is possible to foresee cases where a larger number of electrons could be involved, as when the SOMO is degenerate and has more than one electron.

**Acknowledgment.** F.M. and J.J.N. were supported by the Spanish Science and Education Ministry (BQU2002-04587-C02-02, UNBA05-33-001 and MAT2008-02032/MAT) and the CIRIT (2001SGR-0044 and 2005-PEIR-0051/69). Computer time was also provided by CESCA and BSC. J.S.M. was supported in part by the U.S. NSF (Grant No. 0553573) and the DOE (Grant No. DE FG 03-93ER45504).

**Supporting Information Available:** Figure showing a two-dimensional view of the computed total electron density of the phenalenyl dimer, along the plane that contains the central C atoms of both phenalenyl fragments, and locates the bond critical point. This material is available free of charge via the Internet at <http://pubs.acs.org>.

JA9002298

(33) The AIM analysis of  $\mathbf{1}_2$  was done on the singlet electron density computed at the CASSCF(2,2)/3-21G(d) level, while that in  $\mathbf{1}_2(\text{N}_2)$  was using the ROMP2/3-21G(d) wavefunction. Note that the closed-shell singlet state is the only state where a long-bond can exist according to Lewis electron pairing model. The geometry of the  $\mathbf{1}_2$  dimer was the experimental one in reference,<sup>2</sup> while that of the  $\mathbf{1}_2(\text{N}_2)$  dimer was that indicated above.